Applied Surface Science Advances 11 (2022) 100312

Contents lists available at ScienceDirect

Applied Surface Science Advances

journal homepage: www.sciencedirect.com/journal/applied-surface-science-advances

Synthesis of free-standing graphene in atmospheric pressure microwave plasma for the oil-water separation application

Muhammad Adeel Zafar, Mohan V Jacob *

Electronics Materials Lab, College of Science and Engineering, James Cook University, Townsville, QLD 4811, Australia

ARTICLE INFO

Keywords:
Atmospheric pressure microwave plasma
Free-standing graphene
Methane-derived graphene
Raman spectrum
Scanning electron microscopy of graphene

ABSTRACT

The synthesis of free-standing graphene in a microwave plasma at ambient conditions is currently of great interest. The past works have relied on the usage of higher microwave powers to synthesize free-standing graphene which is not only costly but also an obstacle to the industrialization of the process. The aim of this work was to bring down the cost of the process by synthesizing graphene at a significantly lower microwave power, i.e. 250 W. The formation of graphene was confirmed through Raman spectrum and scanning electron microscopy, where the Raman spectrum showed the signature 2D peak of graphene, and the vertical orientation of the graphene was observed in the microscopic images. The application of graphene in oil-water separation is demonstrated based on its hydrophobic and oleophilic properties. The as-synthesized pristine graphene coated on a melamine sponge showed a mass absorption capacity (57 g/g) comparable to that of functionalized or composite graphene.

Introduction

Graphene is a monatomic layer of graphite, comprised of sp^2-hybridized carbon atoms arranged in a honeycomb structure. In the last two decades, graphene is one of the extensively researched 2-D materials [1]. It is due to its myriad of fascinating properties which include extraordinary mechanical and electrical properties, thermal conductivities, chemical inertness, and optical transparency [2]. Its applications can be found in various fields, for example, electronic devices, energy generation and storage, optical devices, chemical, and biological sensors, etc. [3–7].

Many methods have been developed by researchers to fabricate this promising novel nanomaterial. However, the techniques reported until now involve laborious procedures and require multiple stages of synthesis. For instance, the commonly used chemical exfoliation method, modified Hummers' method [8], demands numerous steps of synthesis such as dilution, mixing, oxidation, washing, centrifuging, and intense stirring [9]. On the other hand, chemical vapor deposition (CVD) [10] and plasma-enhanced chemical vapor deposition (PECVD) [11,12] have many procedural requirements such as high vacuum and temperatures, post-synthesis treatment, and above all they are lengthy processes [12–14].

Atmospheric pressure microwave plasma (APP), which recently gained scientists' attention, can synthesize graphene in a single-step without the need for a catalyst or substrate. Since the operation of atmospheric pressure microwave plasma does not require any vacuuming or heating owing to the synthesis being carried out under ambient-conditions, the cost effectiveness of the process is remarkable [15]. Moreover, due to the free-standing nature of the graphene and continuous synthesis procedure, the yield of the process is higher and scalable. The APP have produced good quality monolayer to few-layer graphene nanosheets from different resources, such as methane, ethanol, aniline, etc. [16–23].

Methane, which is one of the cheap and abundant resources has been widely used in graphene synthesis in CVD or PECVD [24,25]. However, its utilization in APP is scarcely reported. Methane, due to its gaseous form, makes it convenient to actively control its flow on the one hand, and on the other hand, unlike liquid precursors, it eliminates the need for aerosol formation. In APP, Tatarova et al. [18] and Bundaleska et al. [21] used methane to synthesize graphene in two separate studies. They used microwave power as high as 1 kW. In Tatarova et al.'s [18] work, they observed non-uniformity in the structures and also observed particles-like structures. Singh et al. [26] also synthesized graphene from methane at a high microwave power of 1.3 kW and supplied additional hydrogen gas along with methane precursor.

In the current study, our goal was to synthesize graphene using atmospheric pressure microwave plasma (APP) at a low microwave power. We synthesized graphene from methane at a microwave power of

* Corresponding author.
E-mail address: mohan.jacob@jcu.edu.au (M.V. Jacob).

https://doi.org/10.1016/j.apsadv.2022.100312
Received 23 June 2022; Received in revised form 14 September 2022; Accepted 28 September 2022
Available online 7 October 2022

250 W, which is four times lesser than the previously reported methods. A comparison between both, high and low-power synthesized graphene has been made through Raman and SEM analysis. The market mainly relies on the graphene produced by the time-consuming (many hours) Hummers' method. However, APP could be used to synthesize graphene within seconds. Considering that the synthesis is carried out at low microwave power which makes the process energy-efficient, our approach will be highly sought-after in the market. Since the spillage of the oil in the water has detrimental effects on the environment [27], we used as-synthesized graphene in oil-water separation application using the physical absorption method. The coating of as-fabricated pristine graphene, on melamine foam behaved in a similar manner to the nanocomposite of graphene as well as the ones synthesized using additional steps of functionalization.

Materials and method

Materials

Methane and argon gases in ultra-high purity grade were purchased from BOC, Australia. Melamine foam was procured from Bunnings, Australia.

Synthesis of graphene

The synthesis of graphene was carried out using downstream microwave plasma at atmospheric conditions. The setup primarily consists of a microwave generator (2.45 GHz), matching network, quartz tube (30 mm OD), and a sliding short circuit. The microwave generator and the quartz tube were fitted with a water- and air-cooling system respectively. Methane (CH_4) was utilized in its pure form as the only precursor for synthesis. The top end of the quartz tube was enclosed, and it was fitted with the hoses for the supply of argon and methane gasses. The bottom open end of the tube was enabled the expulsion of the reaction gasses.

Argon and methane gasses were fed into the quartz tube separately and continuously at the rate of 3000 and 2500 sccm respectively for 4 min. The graphene is produced straightaway in the plasma reactor once the methane is introduced into the system. The formation takes place on the walls of the quartz tube. However, it can also be collected directly on different substrates for characterizations. Optical microscopic images of graphene, collected on silicone substrate are shown in Fig. S1. Graphene tends to be chemically inert and stable at atmospheric conditions [28]. A study on the thermal stability showed structural defects after 1000°C [29,30]. A basic schematic illustration of the synthesis is shown in Fig. 1.

A combination of low and high microwave power, i.e. 250 W and 500 W, respectively were investigated. The graphene grown was collected directly on silicon substrate for characterizations. Confocal laser Raman spectroscopy (Witec, 532 nm laser) and scanning electron microscopy (SEM) (Hitachi SU 5000) were used to investigate respectively the material's structure and morphology.

Preparation of graphene-coated foam

The graphene, used for melamine foam coating in oil-water separation was synthesized using 250 W microwave power. It was chosen because its synthesis procedure involved low energy requirements. Moreover, the differences in the characteristics of both, low and high power graphene were quite trivial. For the coating, a 1 mg/mL solution of graphene in ethanol was prepared. The solution was ultra-sonicated for 15 min to obtain uniform dispersion of graphene in ethanol. For the purpose of experimentation, only a small sized (~1×1 cm) melamine foam was used. However, the foam can be scaled to any size. To coat the melamine foam with graphene, it was soaked in the solution for 10 min. After soaking, the foam was dried in air to evaporate ethanol. The coated and uncoated melamine foams are shown in Fig. 2.

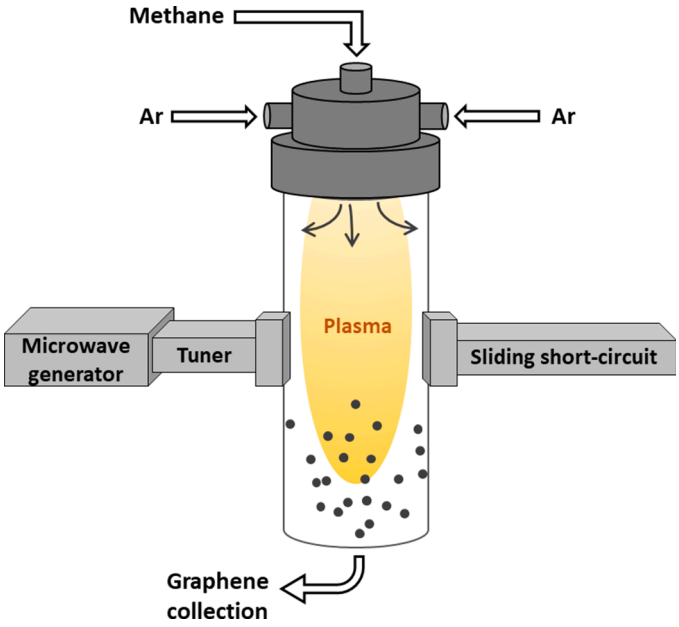

Fig. 1. A schematic illustration of graphene synthesis in atmospheric pressure microwave plasma.

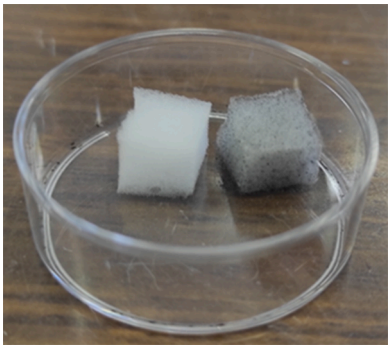

Fig. 2. Image of pristine (left) and graphene-coated (right) melamine foams.

Measurement of water contact angle and oil absorption capacity

The static contact angle was determined by employing KSV CAM 101 optical contact angle device. The wettability of pristine and graphene-coated melamine foam was measured using water and olive oil liquids.

To find out the oil absorption capacity of graphene-coated melamine, a solution of olive oil and water was prepared. The oil in the container formed a layer on the top of the water. The absorption capacity of the graphene-coated melamine foam was measured by gravimetric analysis. The mass absorption capacity was measured by the following formula.

$$Q = \frac{\mathrm{Wt} - \mathrm{Wi}}{Wt} \quad (1)$$

Where Wi and Wt are the weights of the foams before and after oil absorption respectively.

Results and discussions

The as-synthesized graphene nanosheets were analysed using Raman spectroscopy to investigate the structural quality. The Raman spectra of both 250 and 500 W samples, showed three vibrational modes, which are characteristic of graphene materials. They are denoted as D peak (at ~1335 cm^{-1}), G peak (at ~1575 cm^{-1}), and a 2D peak (at ~2675 cm^{-1}), which represent defect mode, vertical vibration mode, and two-

phonon vibration mode, respectively [31]. The Raman spectra are shown in Fig. 3. It is clear from Fig. 3 that graphene has been obtained at both powers. Overall, no significant differences have been observed between both spectrums. In comparison to the 500 W sample, the 250 W sample showed a slightly higher intensity ratio of D and G peak, i.e. I_D/I_G. Similarly, a trivial increase in I_{2D}/I_G and full width at half-maximum (FWHM) values can be observed in the 250 W sample, given in Table 1.

The D peak in the Raman spectrum is indicative of the degree of disorder in a material. This disorder can be due to non-hexagonal rings, dopants, and/or functional groups [32]. The low values of I_D/I_G ratios in our samples show comparatively fewer disorders in the structures. Since this synthesis is under atmospheric conditions, therefore, a slight increase of I_D/I_G ratio in the 250 W sample compared to the 500 W sample, is most likely due to the higher content of oxygen functional groups attached to the basal plane of graphene. In Tatarova et al.'s [18] work, where they synthesized graphene from methane at a microwave power of 1 kW, the intensity values of D and G peaks were nearly the same. They attributed this intense D peak to sp^3-bonded carbon atoms and/or edge effects. Given this, our samples exhibited comparatively less disorder due to relatively smaller I_D/I_G values. Additionally, our samples were synthesized at fairly low microwave power.

The 2D peak in the Raman spectrum is notable. The full width at half-maximum (FWHM) of a 2D peak, and intensity ratio between 2D and G peak (I_{2D}/I_G), are normally associated with the number of layers in graphene. The I_{2D}/I_G values of 2 or higher with FWHM of ~30 cm^{-1}, and I_{2D}/I_G ratios between 1 to 1.5 with FWHM of ~50 cm^{-1} are generally linked with the monolayer and bilayer structures, respectively [33,34]. In this study, for instance, 250 W sample exhibited I_{2D}/I_G and FWHM values of 0.91 and 63 cm^{-1} respectively, which can be suggestive of a few layers of graphene. In Singh et al. [26] work, where they synthesized graphene from methane at 1.3 kW power, the reported I_{2D}/I_G values are around 0.3. Whereas, our samples showed relatively higher values of I_{2D}/I_G, which is an indication of a smaller number of layers than that of their samples.

The low and high-resolution SEM images of the graphene nanosheets deposited directly on silicon substrates are shown in Fig. 4. Both samples showed three-dimensional islands similar to crumpled and torn paper sheets spread on a surface. These islands consisted mainly of a few-layered graphene as discussed in Raman spectra analysis. Apparently, there are no significant differences in SEM images of both samples, except that the 500 W sample has relatively dense islands due to the aggregation of graphene nanostructures. The SEM results are comparable with the reports [21,35,36], where they also synthesized free-standing graphene under atmospheric conditions.

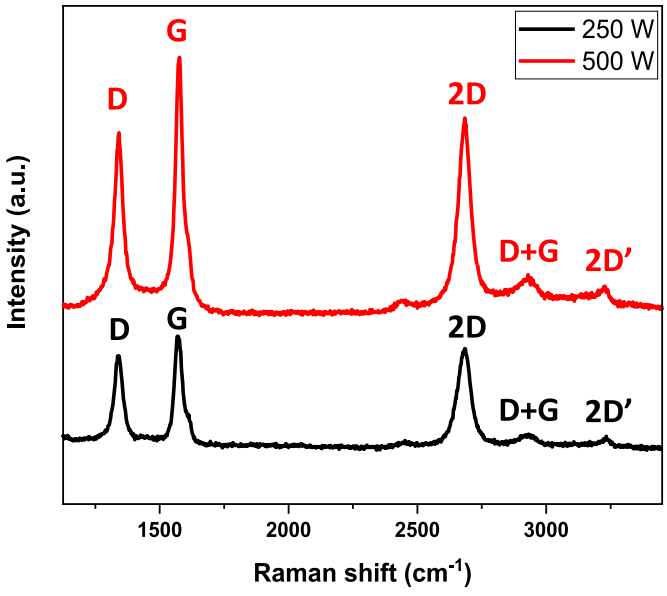

Fig. 3. Raman spectra of 250 and 500 W samples.

Table 1
Intensity ratios and FWHM from Raman spectra.

Microwave power (W)	I_D/I_G	I_{2D}/I_G	FWHM of 2D (cm^{-1})
250	0.88	0.91	63
500	0.83	0.87	57

The growth, morphology and density of graphene mainly depends on the parameters such as microwave power, flow rate of the precursor and the carrier gas. The proposed growth mechanism of our vertical graphene samples can be divided into three stages. It includes nucleation and nanoislands formation on the substrate, growth initiation of graphene nanosheets, and the further growth of graphene. Malesevic et al. [37] and Zhang et al. [38] have reported similar growth proposition. Before the nucleation of graphene, a layer of buffer was formed on the substrate, and this buffer layer subsequently resulted in the nucleation of the graphene.

Water and oil contact angle analysis

Water contact angles of pristine and graphene-coated melamine foam were measured using water and olive oil (shown in Figs. 5 and 6). The droplets of water and oil, 5uL each were used for this purpose. The distance between syringe and foam was kept constant at 20 mm for all the measurements. The pristine foam (Fig. 5a, b) immediately absorbed the water droplet as soon as it dropped onto the foam. Whereas the graphene coating imparted the hydrophobic property in the foam, and hence a water contact angle of 78° was observed (Fig. 5c, d). The hydrophobic property in the foam is highly desirable to avoid any absorption of the water in the oil-water separation process. On the other hand, a high absorption capacity for the oil is required. The contact angles for the oil droplet are shown in Fig. 6. The graphene-coated foam absorbed the oil droplet as soon as it dropped on the foam (Fig. 6c, d). While, the absorption on the pristine foam was very slow, and it showed a high contact angle of 64° even after 10 s (Fig. 6a, b). This characterization shows the oleophilic property of the graphene, highly necessary in the oil-water separation process.

Absorption properties of graphene-coated foam

The oil absorption capacity of the graphene-coated foam was investigated by an experiment shown in Fig. 7. Simply the foam was dipped into the solution of water and oil in which oil was settled at the top. After 5 min of dipping, the foam was taken out. Good absorption of the oil from the water in a container can be seen. The percentage of absorption capacity was determined using Eq. (1). A 57 g/g of absorption capacity was calculated. Comparison of our graphene-coated melamine foam with the previous works is presented in Table 1. In those studies, the preparation of graphene involves several hours of synthesis procedure. Moreover, the graphene used in previous works is either reduced-graphene (contains oxygen functional groups) or functionalized with other materials [39,40]. Whereas, in this work we used pristine graphene, synthesized in few seconds using the microwave plasma and ambient conditions for synthesis. It should also be noted that the foam dipping time in the solution and the coating amount of graphene on the foam has significant effects on the absorption properties. Thus, we believe that a higher concentration of the graphene solution can increase the hydrophobic and oleophilic properties even more.

Non-toxicity and reusability of graphene-coated melamine foam

Graphene is hydrophobic in nature and insoluble in water [46]. As evident in Fig. 7, the residual water after oil absorption is clean and free

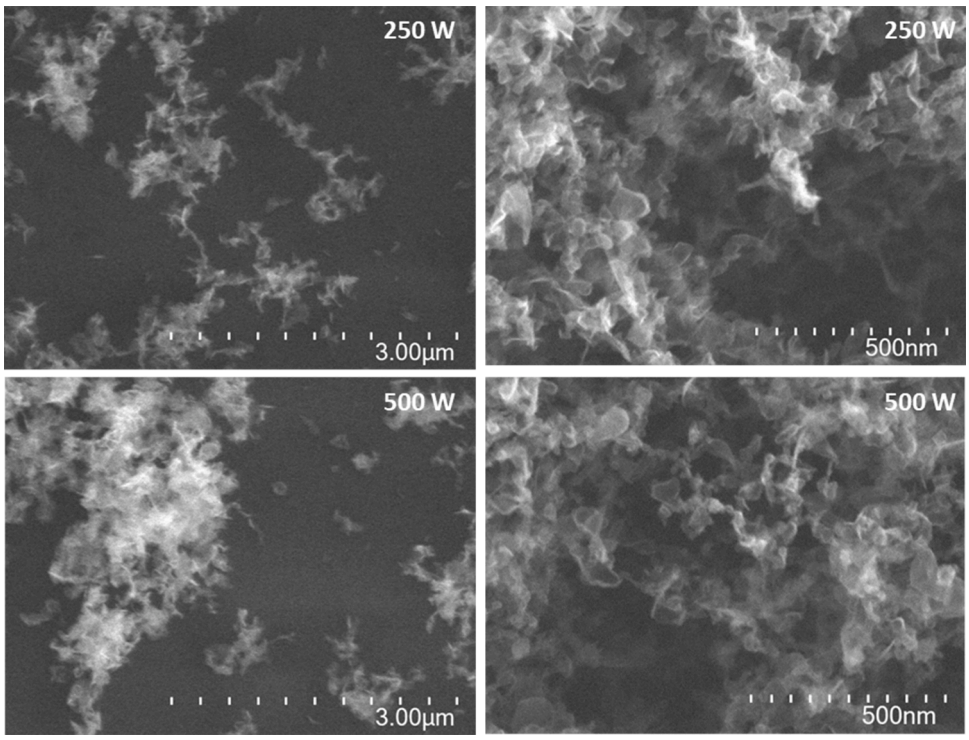

Fig. 4. SEM images of 250 and 500 W graphene samples at lower and higher magnifications.

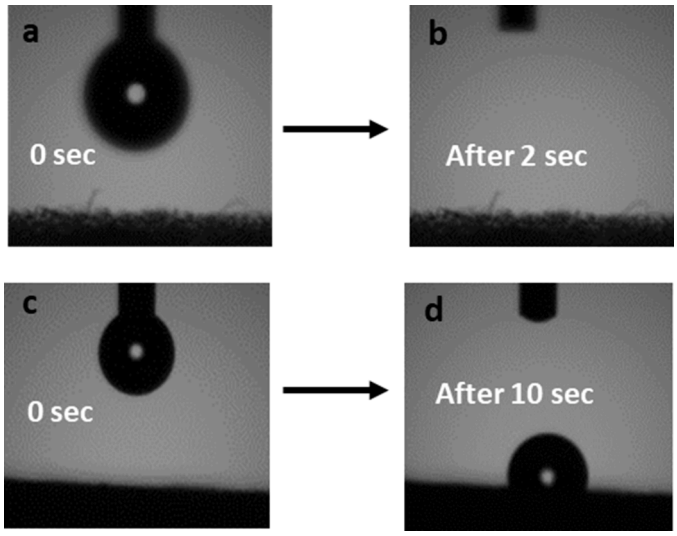

Fig. 5. Water contact angles for (a, b) pristine and (c, d) graphene-coated melamine foams.

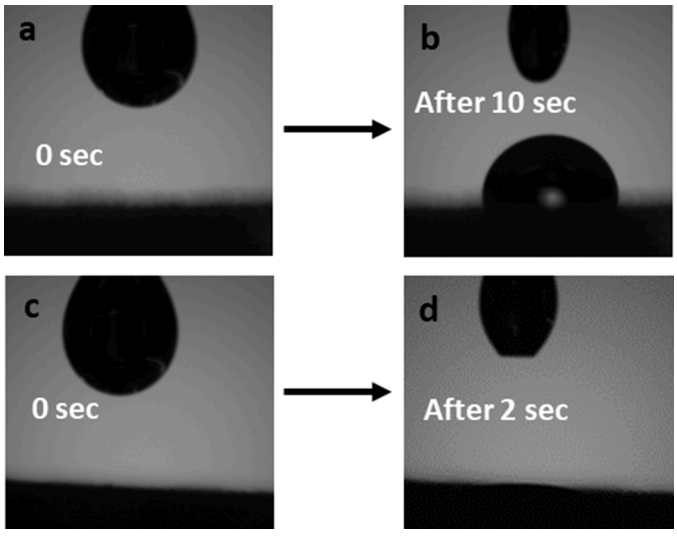

Fig. 6. Oil contact angles for (a, b) pristine and (c, d) graphene-coated melamine foams.

from graphene nanoparticles. Likewise, the poor solubility of melamine in water is also well-known [47,48]. These features of graphene and melamine make them safe for use in oil-water separation application. Moreover, the graphene-coated melamine foam can be reused after squeezing-out the absorbed oil. It allows the recycling of the foam multiple times for oil-water separation. Additionally, melamine foam has been used as a raw material in pyrolysis for the synthesis of nitrogen-doped carbon to be used in batteries [49]. Thus, the choice of foam and coating material in this application is not only suitable for oil-water separation but also provides a valuable resource for future applications.

Conclusion

In a summary, we synthesized graphene from methane using microwave plasma under ambient conditions. The feasibility of the synthesis of graphene at a remarkably low microwave power of 250 W is substantiated in this manuscript. For the fabrication of graphene as reported in this manuscript, there is no need for vacuum and external heating. In addition to that, the method allows for quick fabrication of graphene. The fabrication time is less than 1 min. We have fabricated 1.53 mg/min graphene. The Raman spectra showed lower I_D/I_G and higher I_{2D}/I_G values in comparison to those in literature, where synthesis power was 1 kW or higher. The SEM images showed a crumpled and torn paper-like structure, which is consistent with the previous reports. So

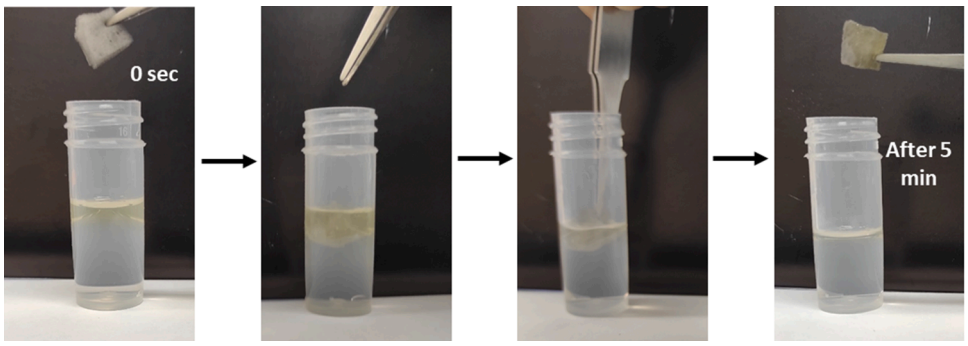

Fig. 7. A series of figures for the absorption of oil from the water using graphene-coated melamine foam.

Table 2
Comparison of graphene-coated foams performance in oil-water separation application.

Materials	Graphene synthesis technique and synthesis time	Absorbed substance	Absorbance capacity (g/g)	Refs.
Silanized graphene polyurethane (PU) sponge	Wet method, several hours	Diesel oil	26	[41]
Functionalized reduced graphene oxide (rGO) PU sponge	Modified Hummer's method, several hours	Pump oil	30	[42]
Graphene coated PU sponge	Modified Hummer's method, several hours	Lubricate oil	32	[43]
rGO coated PU sponge	Modified Hummer's method, several hours	Soybean oil	37.6	[39]
rGO/melamine sponge	Commercially procured	Olive oil	60	[40]
Ag/rGO/melamine sponge	Commercially procured	Soybean oil	40	[40]
Graphene aerogel	Hummer's method, several hours	Vegetable oil	50	[44]
Polybenzoxazine/ reduced graphene oxide wrapped-cellulose sponge	Commercially procured	Crude oil	61.1	[45]
Pristine graphene/ melamine sponge	Atmospheric pressure microwave plasma, few seconds	Olive oil	57	This work

overall, the fabrication method is cheaper, facile, sustainable, and quicker. The as-synthesized graphene was used in oil-water separation application. Graphene-coated melamine foam showed excellent hydrophobic and oleophilic properties, which made graphene an ideal material in the oil-water separation process.

Declaration of Competing Interest

The authors declare that they have no known competing financial interests or personal relationships that could have appeared to influence the work reported in this paper.

Data availability

Data will be made available on request.

Acknowledgments

M.A.Z. gratefully acknowledges financial support through the Australian Government International Research Training Program Scholarship (IRTPS).

Supplementary materials

Supplementary material associated with this article can be found, in the online version, at doi:10.1016/j.apsadv.2022.100312.

References

[1] A.K. Geim, K.S. Novoselov, The rise of graphene, in Nanoscience and technology: a collection of reviews from nature journals, World Scientific, 2010, pp. 11–19.
[2] K.S. Novoselov, et al., Two-dimensional gas of massless Dirac fermions in graphene, Nature 438 (7065) (2005) 197–200.
[3] M.V. Jacob, et al., Catalyst-Free Plasma Enhanced Growth of Graphene from Sustainable Sources, Nano Lett. 15 (9) (2015) 5702–5708.
[4] R.S. Edwards, K.S. Coleman, Graphene synthesis: relationship to applications, Nanoscale 5 (1) (2013) 38–51.
[5] Y. Zhu, D.K. James, J.M. Tour, New routes to graphene, graphene oxide and their related applications, Adv. Mater. 24 (36) (2012) 4924–4955.
[6] P. Rawat, et al., Emergence of high-performing and ultra-fast 2D-graphene nano-biosensing system, Mater. Lett. 308 (2022), 131241.
[7] P.K. Sharma, et al., Ultrasensitive and reusable graphene oxide-modified double-interdigitated capacitive (DIDC) sensing chip for detecting SARS-CoV-2, ACS Sens. 6 (9) (2021) 3468–3476.
[8] N. Zaaba, et al., Synthesis of graphene oxide using modified hummers method: solvent influence, Proc. Eng. 184 (2017) 469–477.
[9] A.T. Smith, et al., Synthesis, properties, and applications of graphene oxide/ reduced graphene oxide and their nanocomposites, Nano Mater. Sci. 1 (1) (2019) 31–47.
[10] Y. Miyasaka, A. Nakamura, J. Temmyo, Graphite thin films consisting of nanograins of multilayer graphene on sapphire substrates directly grown by alcohol chemical vapor deposition, Jpn. J. Appl. Phys. 50 (4S) (2011) 04DH12.
[11] T. Terasawa, K. Saiki, Synthesis of Nitrogen-Doped Graphene by Plasma-Enhanced Chemical Vapor Deposition, Jpn. J. Appl. Phys. 51 (5) (2012).
[12] A. Al-Jumaili, et al., Bactericidal Vertically Aligned Graphene Networks Derived from Renewable Precursor, Tanso Sen'i no Saisentan Gijutsu (2022), 100157.
[13] F. Hadish, et al., Functionalization of CVD grown graphene with downstream oxygen plasma treatment for glucose sensors, J. Electrochem. Soc. 164 (7) (2017) B336.
[14] Y. Liu, Y.M. Chen, Synthesis of large scale graphene oxide using plasma enhanced chemical vapor deposition method and its application in humidity sensing, J. Appl. Phys. 119 (10) (2016), 103301.
[15] A. Dato, et al., Substrate-free gas-phase synthesis of graphene sheets, Nano Lett. 8 (7) (2008) 2012–2016.
[16] A. Dato, Graphene synthesized in atmospheric plasmas—a review, J. Mater. Res. 34 (1) (2019) 214–230.
[17] O. Jašek, et al., Study of graphene layer growth on dielectric substrate in microwave plasma torch at atmospheric pressure, Diamond Relat. Mater. 105 (2020), 107798.
[18] E. Tatarova, et al., Microwave Plasmas Applied for Synthesis of Free-Standing Carbon Nanostructures at Atmospheric Pressure Conditions, J. Magnetohydrodyn. Plasm. Res. 21 (2) (2016) 185.
[19] D. Tsyganov, et al., On the plasma-based growth of 'flowing'graphene sheets at atmospheric pressure conditions, Plasma Sources Sci. Technol. 25 (1) (2015), 015013.
[20] A. Münzer, et al., All gas-phase synthesis of graphene: Characterization and its utilization for silicon-based lithium-ion batteries, Electrochim. Acta 272 (2018) 52–59.

[21] N. Bundaleska, et al., Microwave plasma enabled synthesis of free standing carbon nanostructures at atmospheric pressure conditions, Phys. Chem. Chem. Phys. 20 (20) (2018) 13810–13824.
[22] R. Rincón, et al., Synthesis of multi-layer graphene and multi-wall carbon nanotubes from direct decomposition of ethanol by microwave plasma without using metal catalysts, Plasma Sources Sci. Technol. 24 (3) (2015), 032005.
[23] M.A. Zafar, et al., Single-step synthesis of nitrogen-doped graphene oxide from aniline at ambient conditions, ACS Appl. Mater. Interfaces (2022).
[24] N.-C. Yeh, et al., Single-step growth of graphene and graphene-based nanostructures by plasma-enhanced chemical vapor deposition, Nanotechnology 30 (16) (2019), 162001.
[25] J.-b. Wang, et al., A review of graphene synthesisatlow temperatures by CVD methods, New Carbon Mater. 35 (3) (2020) 193–208.
[26] M. Singh, et al., Effect of hydrogen concentration on graphene synthesis using microwave-driven plasma-mediated methane cracking, Carbon 143 (2019) 802–813.
[27] C. Ji, et al., High performance graphene-based foam fabricated by a facile approach for oil absorption, J. Mater. Chem. A 5 (22) (2017) 11263–11270.
[28] L. Liao, H. Peng, Z. Liu, Chemistry Makes Graphene beyond Graphene, J. Am. Chem. Soc. 136 (35) (2014) 12194–12200.
[29] F. Liu, et al., Thermal stability of graphene in inert atmosphere at high temperature, J. Solid State Chem. 276 (2019) 100–103.
[30] H.Y. Nan, et al., The thermal stability of graphene in air investigated by Raman spectroscopy, J. Raman Spectrosc. 44 (7) (2013) 1018–1021.
[31] B. Liu, et al., N-doped graphene with low intrinsic defect densities via a solid source doping technique, Nanomaterials 7 (10) (2017) 302.
[32] D. Li, et al., Facile synthesis of nitrogen-doped graphene via low-temperature pyrolysis: the effects of precursors and annealing ambience on metal-free catalytic oxidation, Carbon 115 (2017) 649–658.
[33] Y. Hao, et al., Probing layer number and stacking order of few-layer graphene by Raman spectroscopy, Small 6 (2) (2010) 195–200.
[34] C.R.S.V. Boas, et al., Characterization of nitrogen doped graphene bilayers synthesized by fast, low temperature microwave plasma-enhanced chemical vapour deposition, Sci. Rep. 9 (1) (2019) 1–12.
[35] J. Toman, et al., On the transition of reaction pathway during microwave plasma gas-phase synthesis of graphene nanosheets: from amorphous to highly crystalline structure, Plasma Processes Polym. (2021), e2100008.
[36] N. Bundaleska, et al., Large-scale synthesis of free-standing N-doped graphene using microwave plasma, Sci. Rep. 8 (1) (2018) 1–11.
[37] A. Malesevic, et al., Synthesis of few-layer graphene via microwave plasma-enhanced chemical vapour deposition, Nanotechnology 19 (30) (2008).
[38] L. Zhang, et al., Understanding the growth mechanism of vertically aligned graphene and control of its wettability, Carbon 103 (2016) 339–345.
[39] C. Xia, et al., Facile one-pot synthesis of superhydrophobic reduced graphene oxide-coated polyurethane sponge at the presence of ethanol for oil-water separation, Chem. Eng. J. 345 (2018) 648–658.
[40] S. Sun, et al., A bifunctional melamine sponge decorated with silver-reduced graphene oxide nanocomposite for oil-water separation and antibacterial applications, Appl. Surf. Sci. 473 (2019) 1049–1061.
[41] S. Zhou, et al., One-pot synthesis of robust superhydrophobic, functionalized graphene/polyurethane sponge for effective continuous oil–water separation, Chem. Eng. J. 302 (2016) 155–162.
[42] R. Tjandra, et al., Introduction of an enhanced binding of reduced graphene oxide to polyurethane sponge for oil absorption, Ind. Eng. Chem. Res. 54 (14) (2015) 3657–3663.
[43] R. Wu, et al., One-pot hydrothermal preparation of graphene sponge for the removal of oils and organic solvents, Appl. Surf. Sci. 362 (2016) 56–62.
[44] K. Hu, T. Szkopek, M. Cerruti, Tuning the aggregation of graphene oxide dispersions to synthesize elastic, low density graphene aerogels, J. Mater. Chem. A 5 (44) (2017) 23123–23130.
[45] Y. Qin, et al., Mechanically robust polybenzoxazine/reduced graphene oxide wrapped-cellulose sponge towards highly efficient oil/water separation, and solar-driven for cleaning up crude oil, Compos. Sci. Technol. 197 (2020), 108254.
[46] Q.G. Jiang, et al., Reversible Transition of Graphene from Hydrophobic to Hydrophilic in the Presence of an Electric Field, J. Phys. Chem. C 116 (36) (2012) 19321–19326.
[47] Y. Wu, et al., Monodispersed or narrow-dispersed melamine–formaldehyde resin polymer colloidal spheres: preparation, size-control, modification, bioconjugation and particle formation mechanism, J. Mater. Chem. B 1 (2) (2013) 204–212.
[48] K.G. Chattaraj, S. Paul, Understanding of structure and thermodynamics of melamine association in aqueous solution from a unified theoretical and experimental approach, J. Chem. Inf. Model. 58 (8) (2018) 1610–1624.
[49] L. Zhang, et al., Direct pyrolysis of melamine sponge toward nitrogen-doped carbon for high-performance lithium and sodium ion storage, J. Alloys Compd. 760 (2018) 84–90.